Magnetization and Microstructure Dynamics in Fe/MnAs/GaAs(001): Fe Magnetization Reversal by a Femtosecond Laser Pulse

C. Spezzani, E. Ferrari, E. Allaria, F. Vidal, A. Ciavardini, R. Delaunay, F. Capotondi, E. Pedersoli, M. Coreno, C. Svetina, L. Raimondi, M. Zangrando, R. Ivanov, I. Nikolov, A. Demidovich, M. B. Danailov, H. Popescu, M. Eddrief, G. De Ninno, M. Kiskinova, and M. Sacchi

Phys. Rev. Lett. **113**, 247202 — Published 9 December 2014

DOI: 10.1103/PhysRevLett.113.247202

Magnetization and microstructure dynamics in Fe/MnAs/GaAs(001): Fe magnetization reversal by a femtosecond laser pulse

C. Spezzani[1], E. Ferrari[1,2], E. Allaria[1], F. Vidal[3,4], A. Ciavardini[5], R. Delaunay[6,7], F. Capotondi[1], E. Pedersoli[1], M. Coreno[1,5], C. Svetina[1,8], L. Raimondi[1], M. Zangrando[1], R. Ivanov[1,†], I. Nikolov[1], A. Demidovich[1], M. Danailov[1], H. Popescu[9], M. Eddrief[3,4], G. De Ninno[1,10], M. Kiskinova[1], M. Sacchi[3,4,9,*]

[1] *ELETTRA – Sincrotrone Trieste, 34149 Trieste, Italy*

[2] *Università degli Studi di Trieste, Dipartimento di Fisica, 34127 Trieste, Italy.*

[3] *Sorbonne Universités, UPMC Univ Paris 06, UMR 7588, INSP, F-75005, Paris, France*

[4] *CNRS, UMR 7588, Institut des NanoSciences de Paris, F-75005, Paris, France*

[5] *CNR – ISM, via Salaria km 29,300 –00016 Monterotondo Scalo (RM), Italy*

[6] *Sorbonne Universités, UPMC Univ Paris 06, UMR 7614, LCPMR, F-75005 Paris, France*

[7] *CNRS, UMR 7614, LCPMR, F-75005 Paris, France*

[8] *University of Trieste, Graduate School of Nanotechnology, 34127 Trieste, Italy*

[9] *Synchrotron SOLEIL, L'Orme des Merisiers, Saint-Aubin, France*

[10] *Laboratory of Quantum Optics, University of Nova Gorica, 5001 Nova Gorica, Slovenia*

Thin film magnetization reversal without applying external fields is an attractive perspective for applications in sensors and devices. One way of accomplishing it is by fine tuning the microstructure of a magnetic substrate via temperature control, as in the case of a thin Fe layer deposited on a MnAs/GaAs(001) template. This work reports a time-resolved resonant scattering study exploring the magnetic and structural properties of the Fe/MnAs system, using a 100 fs optical laser pulse to trigger local temperature variations and a 100 fs x-ray free-electron laser pulse to probe the induced magnetic and structural dynamics. The experiment provides direct evidence that a single optical laser pulse can reverse the Fe magnetization locally. It reveals that the time scale of the magnetization reversal is slower than that of the MnAs structural transformations triggered by the optical pulse, which take place after a few ps already.

* Corresponding author. maurizio.sacchi@synchrotron-soleil.fr

Controlling the local magnetization of a thin film without applying an external magnetic field opens up new applications and functionalities for devices. Electron currents [1], polarized light [2] or electric fields [3] have provided new means for acting on the magnetization direction in ferromagnetic systems. Another approach is using active templates, namely self-organized magnetic substrates featuring natural spatial modulations that can be controlled by simply tuning the temperature. A typical example is the intriguing magnetic behavior of thin Fe films controlled by the temperature-driven phase transition of the underlying MnAs/GaAs(001) substrate [4-6]. Fig. 1 sketches the Fe magnetization switching mechanism in Fe/MnAs/GaAs(001) and summarizes some structural and magnetic properties of this system.

The first order phase transition between the ferromagnetic α-phase and the paramagnetic β-phase of MnAs occurring at 40ºC [9] makes it an attractive material for applications in magnetocaloric [7] and spintronic devices [8]. Most appealing is the pattern structure in thin MnAs films grown on GaAs(001), where α and β phases coexist as regular alternating stripes at ambient temperatures [10]. The MnAs thickness **t** determines the period **p** of the stripes; the widths of α and β components vary continuously with temperature over the 10–40ºC range, their sum remaining roughly constant and equal to **p**. The long and narrow α-stripes, with the easy magnetization direction along their short side (see Fig. 1 and ref. [10]), generate dipolar magnetic fields extending outside of the MnAs layer, in particular above its surface where they can reach hundreds of Oe [4,5,11]. Using Fe/MnAs/GaAs(001) samples, it was shown experimentally [4,5,11,12] that it is possible to reverse the direction of the Fe magnetization $\mathbf{M}^{Fe}$ by controlling the MnAs surface dipolar fields associated with the α-β morphology [13]. Modifying $\mathbf{M}^{Fe}$ in a thermal cycle, without making use of an external magnetic field, has potential for temperature-driven magnetization control applications [6].

Here we address the next logical step of this approach, where the energy required for changing the MnAs temperature and attaining local $\mathbf{M}^{Fe}$ switching is provided by an ultrafast optical laser pulse. The $\mathbf{M}^{Fe}$ evolution in response to the laser excitation will depend on the surface dipolar fields generated during the structural modification and recovery of the MnAs template. This is why, in our experiment, we address both the Fe magnetization reversal and the MnAs microstructure dynamics.

The dynamics of α-β stripes in MnAs upon ultra-fast local heating was first studied by UV diffraction [14], showing changes on a timescale as short as ~15 ps. Laser-based experiments [15,16] showed a damped oscillatory behavior of the diffracted intensity up to 10^{-9} s, with a slow recovery of the striped phase within ~10^{-8}–10^{-7} s. The present study makes use of a free-electron-laser (FEL) x-ray probe to show that a single ~100 fs optical laser pulse can

produce local Fe magnetization reversal, on a timescale that we associate with slow MnAs re-thermalization rather than with fast MnAs structural modifications.

The $ZnSe_{4nm}/Fe_{3nm}/MnAs_{200nm}/GaAs(001)$ sample was prepared by molecular beam epitaxy, as described in Refs. [4, 5]. The measurements were performed at the DIPROI beamline [17] of the FERMI FEL source [18], using the vertical-scattering-plane IRMA reflectometer [19]. A thermoelectric device set the static sample temperature $T_\circ$ (-10 – +70°C range) and an electromagnet applied a field along the in-plane MnAs easy magnetization axis (Fig. 1a). The λ=780 nm laser pulses (with fluence F in the 1–30 mJ cm^{-2} range) impinged on the sample at 2° with respect to the FEL beam; the laser spot-size was adjusted to be ~300 μm, i.e. three times that of the FEL radiation. We probed the Fe magnetization and the MnAs structural response after the optical laser pulse using FEL radiation tuned at the Fe 3p→3d resonance (53.7 eV, λ = 23.07 nm). The time delay Δt between the probe and pump pulses, both with ~100 fs duration and 10 Hz repetition rate, could be adjusted from negative values up to 400 ps using an optical delay line. Timing jitter between pump and probe was ~10 fs [20]. The high brilliance and low repetition rate of the FERMI source allowed us to use high fluence pump pulses, all the way keeping the average absorbed power low. Maintaining the initial temperature $T_\circ$ constant for every pump-probe shot is essential to our experiment, since MnAs properties are very sensitive to temperature variations [10]. Under our experimental conditions, the pump excitation depth and the FEL probing depth were ~27 nm and ~20 nm, respectively. We measured magnetic reflectivity in transverse MOKE geometry [21, 22] using linearly p-polarized FEL radiation, with the α-MnAs easy axis normal to the scattering plane. For structural analysis, we scanned the sample angle θ at fixed detector angle ω, in order to vary the projection of the exchanged momentum normal to the MnAs stripes [4, 5].

M^{Fe} reversal by a single femtosecond laser pulse – Fig. 2 shows that, starting from the α-MnAs phase ($T_\circ$ = 5°C, no stripes, as in Fig. 1a), a single 100 fs laser pulse produces local $\mathbf{M}^{Fe}$ reversal. First, a magnetic pulse sets the Fe in its high reflectivity magnetic state, defined as $\mathbf{M}^{Fe+}$ in Fig. 2. Then a single optical laser pulse is let through by using a mechanical chopper; its absorption by the sample produces an abrupt reduction in the reflectivity, corresponding to the Fe magnetization switching towards the $\mathbf{M}^{Fe-}$ state. Scanning the sample under the FEL beam confirms that this change is a local event, occurring only within the pumped region. The fractional magnetization reversal depends strongly on the energy deposited by the optical laser pulse: it is ~75% of the $\mathbf{M}^{Fe}$ saturation value for F = 5–25 mJ cm^{-2} and diminishes quickly below 5 mJ cm^{-2}, till no reversal is observed at F = 1 mJ cm^{-2} [23].

In order to determine the timescale of the laser-induced $\mathbf{M}^{Fe}$ reversal, we implemented a measurement scheme [23] where a magnetic pulse resets the sample magnetization state before each pump-probe sequence. Under these conditions, our reflectivity measurements did not evidence any Fe magnetization reversal within the Δt range spanned by our delay-line, indicating that the laser-induced $\mathbf{M}^{Fe}$ reversal shown in Fig. 2 takes place on a timescale longer than 400 ps [23].

We know that, under static conditions (see Fig. 1), the Fe magnetization reversal is driven by the formation and disappearance of surface dipolar fields related to the α/β stripes [4,5,11]. In the following, we will address the time evolution of the MnAs microstructure, by using the same pump-probe scheme.

Dynamics of the α/β stripes pattern – Fig. 3a shows rocking curves (θ scans at fixed $\omega = 86°$, λ is 23.07 nm) measured at different pump-probe delays starting from the striped MnAs phase ($T_\circ = 21°C$). For $\Delta t < 0$, the 1st and 2nd order Bragg peaks correspond to the regular α/β stripes with period **p**=1340 nm. Their intensities decrease rapidly with Δt, and the evolution of the 1st order position indicates an increasing period **p**. We studied in more detail the dependence of the dynamics on $T_\circ$ and F by measuring the scattered intensities at fixed $\Delta\theta = (\theta-\omega/2)$. The decay of both the 1st and 2nd orders displays two regimes; the simplest fitting function is a double exponential decay (see Fig. 3b), with the time constants t_1 (in the 3–14 ps range) and t_2 (50–250 ps) always differing by more than one order of magnitude. For all the explored $T_\circ$ and F values, 2nd order decays faster than 1st order. With respect to previous studies, Fig. 3b shows that the stripes-related Bragg peaks do not appear ($T_\circ = -2°C$) or strengthen ($T_\circ = 16°C$) after the laser pulse, as it would be expected [10, 24] if one assumes a quasi-static temperature-driven α→β transition [14, 15].

Understanding the time-dependent change in the stripe period **p** requires some support from model calculations. The $\mathbf{p} \approx 5\times\mathbf{t}$ relation derived by Kaganer *et al*. [24] for the MnAs/GaAs(001) system no longer holds in the presence of an overlayer, and additional constraints at the top interface must be accounted for in the energy minimization process that defines the equilibrium **p** value [12]. Defining ξ as the thickness of a top MnAs layer that underwent complete transition to the β-phase, the influence of an increasing ξ on the equilibrium stripe period has two counteracting effects: reducing the phase-coexistence layer thickness (200-ξ) shortens **p**, while increasing the β-overlayer thickness ξ enlarges **p** [8]. The $\mathbf{p}(\xi)$ value that minimizes the system energy is found to increase up to $\xi \sim 50$ nm, then it decreases rapidly till $\xi \sim 100$ nm. For larger ξ values, there is no clear energy minimum as a

function of **p**, indicating that stripes formation is no longer favorable. Although these values obtained under static conditions cannot apply directly to fast dynamics experiments, the calculated **p**(ξ) trend helps interpreting our scattering data.

Fig. 4a shows the Δt dependence of the stripes period **p**, determined by fitting the rocking curves in Fig. 3a, while Fig. 4b shows delay-line scans at fixed $\Delta\theta$ ($T_\circ = 21°C$, striped phase). In both cases, squares and circles refer to peaks at off-specular angles $\Delta\theta \sim 0.7^\circ$ and $\Delta\theta \sim 1.5^\circ$, respectively. When Δt increases, the 1st order peaks move closer to the specular and **p** evolves from 1340 nm at $\Delta t < 0$ to ~1550 nm at $\Delta t \sim 250$ ps (Fig. 4a). A similar trend is observed for the 2nd order peaks up to $\Delta t \sim 100$ ps, where they vanish. The steeper decrease of the 2nd order intensity (Fig. 4b), together with a slight increase in the specular reflectivity (not shown), is consistent [25] with a smoothing of the steps that modulate the scattering surface in the striped phase (Fig. 1b). At $\Delta t \sim 250$ ps, the intensity increases at $\Delta\theta \sim 1.5^\circ$, but the angular position of these well-defined peaks (Fig. 3a) doesn't match 2nd order diffraction from $\mathbf{p} \approx 1550$ nm. We interpret this result as the emergence of a new much shorter order parameter (~600 nm) that sets in between 250 and 350 ps after the laser pulse, in agreement with the **p**(ξ) calculations mentioned above.

Electron-lattice interactions, resulting in a temperature increase that exceeds hundred degrees in a few ps, are the key element for interpreting the evolution of the MnAs microstructure following the laser-pulse excitation. According to Lazÿewski et al. [26], one can also associate the observed structural dynamics with the reduction of the Mn magnetic moment induced by the laser pulse: it is then the spin-lattice coupling, mediated by the soft phonon mode [27], that promotes the $\alpha \rightarrow \beta$ transition. Both electron-lattice and spin-lattice couplings have ps timescales and we cannot single-out their contributions based on our experimental results only. Therefore we associate the shorter timescale t_1 ($\sim 10^{-11}$ s, range 1 in Fig. 4) to the electron-lattice and/or spin-lattice energy exchange processes, leading to the formation of a homogeneous β-phase layer within the irradiated volume. Since the laser pulse is entirely absorbed within a thickness of ~30 nm, the rest of the MnAs layer still features α/β stripes, with their height difference modulating the scattering surface. The local temperature increase and the presence of an all–β layer at the surface smooth this modulation laterally, leading to a faster decrease of the 2nd order Bragg peaks compared to the 1st order ones [25]. Thermal diffusion progressively increases the temperature in deeper layers, moving the (all–β)/(α–β) separation line towards the GaAs substrate. Therefore, we associate the slower decrease of the Bragg peak intensity with characteristic time t_2 ($\sim 10^{-10}$ s, range 2 in Fig. 4) to heat diffusion towards the MnAs/GaAs interface. The concomitant increase of the stripes period until $\Delta t \sim 250$ ps matches our

calculations well. The new much shorter (~600 nm) order parameter revealed over the 250–350 ps range (range 3 in Fig. 4) is consistent with the prediction of a drastic **p** reduction before stripes disappear (time-range 4 in Fig. 4).

Implications for the $\boldsymbol{M}^{Fe}$ *reversal* – Fig. 5 depicts the proposed laser induced magnetization switching mechanism, in analogy with the temperature induced process sketched in Fig. 1. The description of the MnAs microstructural changes given above explains why we never observe the Bragg peak intensity increase: the laser pulse drives a rapid complete transformation of MnAs into the β phase, eliminating ordered stripes when they exist, but never favoring their formation. As shown also by the $T_\circ$ = -2°C curve in Fig. 3b, starting from the α-MnAs homogeneous phase the laser pulse does not induce α/β-stripes formation over the spanned time range (Fig. 5a-c). This result explains why we do not observe $\mathbf{M}^{\mathbf{Fe}}$ reversal up to Δt=400 ps, since, as depicted in Fig. 1b, the process relies on the surface dipolar fields generated by the finite size α-stripes in the phase coexistence region. Using the MnAs parameters [28] and a simple thermal diffusion model [29], we estimated the Δt dependence of the vertical temperature profile over a time range wider than experimentally accessible. The results show that it takes ~5 ns to transform the whole MnAs layer into the β-phase (Fig. 5d) and about ten times longer before it cools again below 40°C, forming ordered α/β stripes (Fig. 5e) and finally leading to $\mathbf{M}^{\mathbf{Fe}}$ reversal at equilibrium (Fig. 5f).

Using FEL resonant scattering we studied the Fe magnetization and the MnAs microstructure dynamics induced in the Fe/MnAs/GaAs(001) sample by ~100 fs optical laser pulses. A distinct finding is that one single laser pulse can reverse the Fe magnetization locally. We show that the MnAs microstructure dynamics involves transformation into the β-phase at ps time scales, characteristic of electron and spin energy transfer to the lattice, followed by slower thermal-diffusion controlled modifications. The microstructural changes relevant to the Fe magnetization reversal, though, do not take place within the 400 ps timespan accessible in our experiment. We infer, based also on model calculations, that, although triggered by a single ultra-short laser pulse, the Fe magnetization reversal is driven not by the fast modifications induced into the MnAs template structure, but by the α/β regular stripes formation that takes place during the return to the equilibrium by slow re-thermalization of the system. In conclusion, although the dynamics of the reversal process could not be explored entirely, our study demonstrates the optical switch of the Fe-overlayer magnetization, clarifying part of the MnAs structural changes that drive it.

We thank the FERMI Commissioning, Laser and Padres teams for dedicated time and support during the experiment. We are grateful to F. Sirotti and M. Marangolo for discussions of the manuscript. R.D., H.P. and M.S. acknowledge financial support from CNRS, via the PEPS_SASLELX program. The FERMI project at Elettra – Sincrotrone Trieste is supported by MIUR under grants FIRB-RBAP045JF2 and FIRB-RBAP06AWK3.

† Present address: DESY Photon Science, Notkestr. **85**, D-22607 Hamburg, Germany

[1] M. Yamanouchi, D. Chiba, F. Matsukura, H. Ohno, Nature **428**, 539 (2004).

[2] A. V. Kimel *et al.*, Nature **435**, 655 (2005).

[3] D. Chiba *et al.*, Nature **455**, 515-518 (2008); M. Saito, K. Ishikawa, S. Konno, K. Taniguchi, T. Arima, Nature Mater. **8**, 634-638 (2009).

[4] M. Sacchi, M. Marangolo, C. Spezzani, L. Coelho, R. Breitwieser, J. Milano, and V. H. Etgens, Phys. Rev. B **77**, 165317 (2008).

[5] M. Sacchi, M. Marangolo, C. Spezzani, R. Breitwieser, H. Popescu, R. Delaunay, B. Rache Salles, M. Eddrief, and V. H. Etgens, Phys. Rev. B **81**, 220401(R) (2010).

[6] M. Marangolo and M. Sacchi, *Method for changing the direction of magnetization in a ferromagnetic layer*, French patent n. 2 947 375 (26/08/2011); US patent pending.

[7] L. Pytlik and A. Zieba, J. Magn. Magn. Mater. **51**, 199 (1985); H. Wada and Y. Tanabe, Appl. Phys. Lett. **79**, 3302 (2001); O. Tegus, E. Brück, K. H. J. Buschow, and F. R. de Boer, Nature **415**, 150 (2002); D. H. Mosca, F. Vidal, and V. H. Etgens, Phys. Rev. Lett. **101**, 125503 (2008); J.-Y. Duquesne, J.-Y. Prieur, J. A. Canalejo, V. H. Etgens, M. Eddrief, A. L. Ferreira, and M. Marangolo, Phys. Rev. B **86**, 035207 (2012).

[8] M. Ramsteiner, H. Y. Hao, A. Kawaharazuka, H. J. Zhu, M. Kastner, R. Hey, L. Daweritz, H. T. Grahn, and K. H. Ploog, Phys. Rev. B **66**, 081304(R) (2002); M. E. Nowakowski, G. D. Fuchs, S. Mack, N. Samarth, and D. D. Awschalom, Phys. Rev. Lett. **105**, 137206 (2010).

[9] B. T. M. Willis and H. P. Rooksby, Proc. Phys. Soc. B **67** 290 (1954); C. P. Bean and D. S. Rodbell, Phys. Rev. **126**, 104 (1962); N. Menyuk, J.A. Kafalas, K. Dwight, and J.B. Goodenough, Phys. Rev. **177**, 942 (1969); Y.-J. Zhao, W. T. Geng, A. J. Freeman, and B. Delley, Phys. Rev. B **65**, 113202 (2002).

[10] M. Tanaka, J. P. Harbison, M. C. Park, Y. S. Park, T. Shin, and G. M. Rothberg, Appl. Phys. Lett. **65**, 1964 (1994); F. Schippan, G. Behme, L. Däweritz, K. H. Ploog, B. Dennis, K.-U. Neumann, and K. R. A. Ziebeck, J. Appl. Phys. **88**, 2766 (2000); R. Magalhães-Paniago, L.N. Coelho, B.R.A. Neves, H. Westfahl, F. Iikawa, L. Däweritz, C. Spezzani, and M. Sacchi,

Appl. Phys. Lett. **86**, 053112 (2005); L. Däweritz, Rep. Prog. Phys. **69**, 2581 (2006); J. Wikberg *et al.*, Phys. Rev. B **83**, 024417 (2011).

[11] R. Breitwieser, M. Marangolo, J. Lüning, N. Jaouen, L. Joly, M. Eddrief, V.H. Etgens, and M. Sacchi, Appl. Phys. Lett. **93**, 122508 (2008).

[12] F. Vidal, C. Spezzani, R. Brietwieser, M. Marangolo, M. Eddrief, M. Sacchi, and V. Etgens, Appl. Phys. Lett. **97**, 251914 (2010).

[13] Extremely weak coupling between Fe and MnAs was inferred from the observation of element selective hysteresis loops with different coercive fields [4,5]. A recent work [D. Demaille, G. Patriarche, C. Helman, M. Eddrief, V. H. Etgens, M. Sacchi, A. M. Llois, and M. Marangolo, Crystal Growth & Design **13**, 4279 (2013)] points to the formation of an antiferromagnetic FeMnAs phase at the Fe/MnAs interface, which may explain an effective decoupling between the two adjacent ferromagnetic layers.

[14] M. Sacchi, C. Spezzani, E. Allaria, E. Ferrari, M. Coreno, M. Marangolo, M. Eddrief, V. Etgens, and G. DeNinno, Appl. Phys. Lett. **100**, 211905 (2012).

[15] J. J. Dean, D. W. Rench, N. Samarth, and H. M. van Driel, Phys. Rev. Lett. **111**, 035701 (2013).

[16] J. J. Dean, C. Lange, and H. M. van Driel, Phys. Rev. B **89**, 024102 (2014).

[17] M. Zangrando *et al.*, Rev. Sci. Instrum. **80**, 113110 (2009) ; E. Pedersoli *et al.*, *ibid.*, **82**, 043711 (2011); F. Capotondi *et al.*, *ibid.*, **84**, 051301 (2013).

[18] E. Allaria *et al.*, Nature Photon. **6**, 699 (2012); *ibid*. **7**, 913 (2013).

[19] M. Sacchi, C. Spezzani, P. Torelli, A. Avila, R. Delaunay, and C. F. Hague, Rev. Sci. Instrum. **74**, 2791 (2003).

[20] M.B. Danailov et al., Optics Express **22**, 12869 (2014); P. Cinquegrana, S. Cleva, A. Demidovich, G. Gaio, R. Ivanov, G. Kurdi, I. Nikolov, P. Sigalotti, and M. B. Danailov, Phys. Rev. ST Accel. Beams **17**, 040702 (2014).

[21] M. Sacchi, G. Panaccione, J. Vogel, A. Mirone, and G. van der Laan, Phys. Rev. B **58**, 3750 (1998); M. Hecker, P. M. Oppeneer, S. Valencia, H. C. Mertins, and C. M. Schneider, J. Electron Spectr. Relat. Phenom. **144-147**, 881 (2005).

[22] C. La-O-Vorakiat *et al.*, Phys. Rev. Lett. **103**, 257402 (2009); Phys. Rev. X **2**, 011005 (2012).

[23] Supplemental Material at http://link.aps.org/supplemental/*xxx* provides further details of the experiment and comments on the partial $\mathbf{M}^{\mathbf{Fe}}$ reversal.

[24] V. M. Kaganer, B. Jenichen, F. Schippan, W. Braun, L. Däweritz, and K. H. Ploog, Phys. Rev. B **66**, 045305 (2002).

[25] P. Mikulík and T. Baumbach, Phys. Rev. B **59**, 7632 (1999).

[26] J. Lazewski, P. Piekarz, J. Tobola, B. Wiendlocha, P. T. Jochym, M. Sternik, and K. Parlinski, Phys. Rev. Lett. **104**, 147205 (2010); J. Lazewski, P. Piekarz, and K. Parlinski, Phys. Rev. B **83**, 054108 (2011).

[27] J. Ihlemann and K. Bärner, J. Magn. Magn. Mater. **46**, 40 (1984); O. Palumbo, C. Castellano, A. Paolone, and R. Cantelli, J. Phys.: Condens. Matter **17**, 1537 (2005); J. D. Zou, H. Wada, B. G. Shen, J. R. Sun, and W. Li, Europhys. Lett. **81**, 47002 (2008).

[28] S. Fujieda, Y. Hasegawa, A. Fujita, and K. Fukamichi, J. Appl. Phys. **95**, 2429 (2004).

[29] e.g., J. H. Bechtel, J. Appl. Phys. **46**, 1585 (1975); J. Hohfield, S.-S. Wellershoff, J. Güdde, U. Conrad, V. Jähnke, and E. Matthias, Chem. Phys**. 251**, 237 (2000).

Figure captions

FIG. 1 (color online). Schematic picture of the temperature driven Fe magnetization reversal in Fe/MnAs/GaAs(001): sketched is a thermal cycle between 5 and 20°C. (a) At the initial temperature of 5°C, Fe and α-MnAs magnetizations are set parallel by a magnetic pulse H_{ext}, applied along the α-MnAs easy magnetization axis (**a** axis of the orthorhombic structure, parallel to GaAs [110]). (b) Increasing the temperature into the phase coexistence region produces stripes running parallel to the MnAs **c**-axis, alternating the α and β phases. Finite size ferromagnetic α-stripes generate dipolar fields extending above the MnAs surface (dashed lines) that act on the Fe overlayer, reversing its magnetization. (c) At the end of the thermal cycle, MnAs recovers its initial configuration, while the Fe layer magnetization has reversed sign [5].

FIG. 2 (color online). Magnetization sensitive specular reflectivity (θ=ω/2=43°) of p-polarized FEL radiation tuned at the Fe-3p resonance ($T_\circ$ = 5°C). A magnetic pulse (300 Oe, 5 ms duration) saturates the Fe magnetization in the high reflectivity state ($\mathbf{M}^{Fe+}$). When a single pump-laser pulse (F=10 mJ cm^{-2}, 100 fs duration) reaches the sample, reflectivity drops towards the $\mathbf{M}^{Fe-}$ value.

FIG. 3 (color online). (a): Rocking scans measured at $T_\circ$ = 21°C (striped phase), showing specular reflectivity (Δθ=0°) and Bragg peaks. Each curve corresponds to an increasing pump-probe delay Δt from -10 ps (▬) to +255 ps (●). (b): 1st order Bragg peak scattered intensity (Δθ=0.7±0.1°) *vs.* Δt, for $T_\circ$ = -2 (■, no stripes), 16 (□) and 34 (○) °C. Lines are double exponential decays with given t_1 and t_2 values. F = 10 mJ cm^{-2}.

FIG. 4 (color online). (a) Order parameters determined from peak positions in Fig. 3a. (b) Normalized scattered intensity *vs.* Δt (squares: Δθ = 0.7 ± 0.1°; circles: Δθ = 1.5 ± 0.1°). For all data, $T_\circ$ = 21°C (striped phase) and F = 10 mJ cm^{-2}. Legend: (■) 1st order, **p** = 1340 – 1550 nm; (○) 2nd order, **p** = 1340 – 1370 nm; (●) 1st order, **p** ~600 nm. Time-ranges 1 to 4 are outlined (see text).

FIG. 5 (color online). Schematic picture of the laser driven Fe magnetization reversal in Fe/MnAs/GaAs(001), analogous to that of Fig. 1 (temperature driven process). Sketched is the local laser excitation of an initial low temperature α-MnAs state, with Fe and MnAs parallel magnetizations. (a) Over the pulse duration time, the laser energy is released to the electrons within the interaction volume. (b) The energy is transferred to the lattice within a few ps, driving the fast MnAs α→β transition within the interaction volume. (c) The α→β transition proceeds towards the GaAs substrate by thermal diffusion, until (d) the entire MnAs layer is in the β phase within a few ns (estimated value). (e) At longer delays the systems cools down again and, after an estimated ~50 ns, goes through the phase-coexistence temperature region; it is during this re-thermalization phase that we expect the Fe magnetization switching to take place. (f) The system approaches its static temperature again, with antiparallel Fe and MnAs magnetizations.

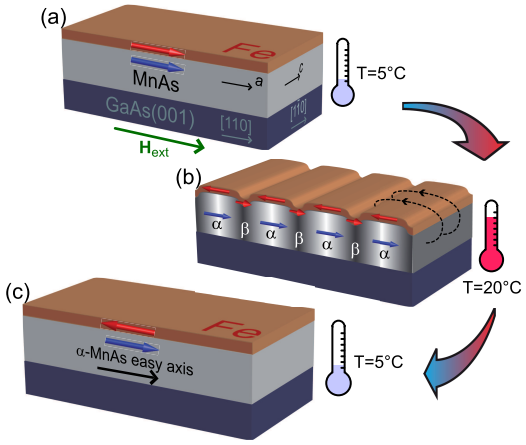

Figure 1 LT14521 03NOV2014

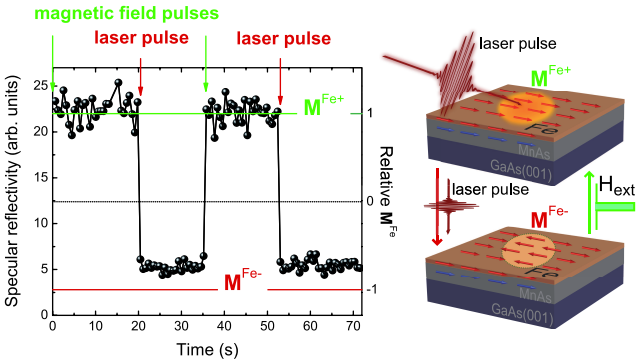

Figure 2 LT14521 03NOV2014

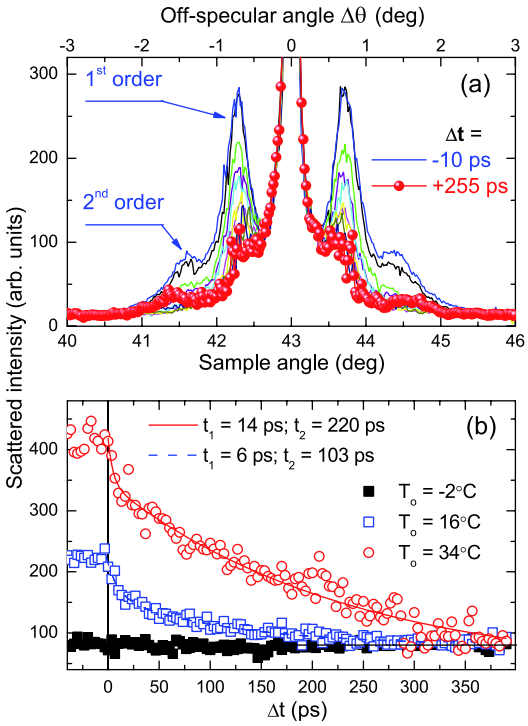

Figure 3 LT14521 03NOV2014

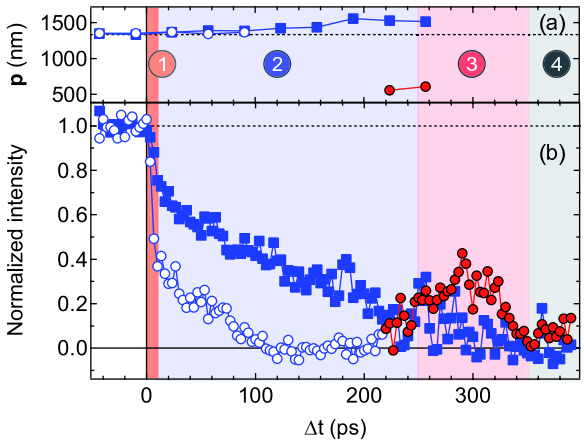

Figure 4 LT14521 03NOV2014

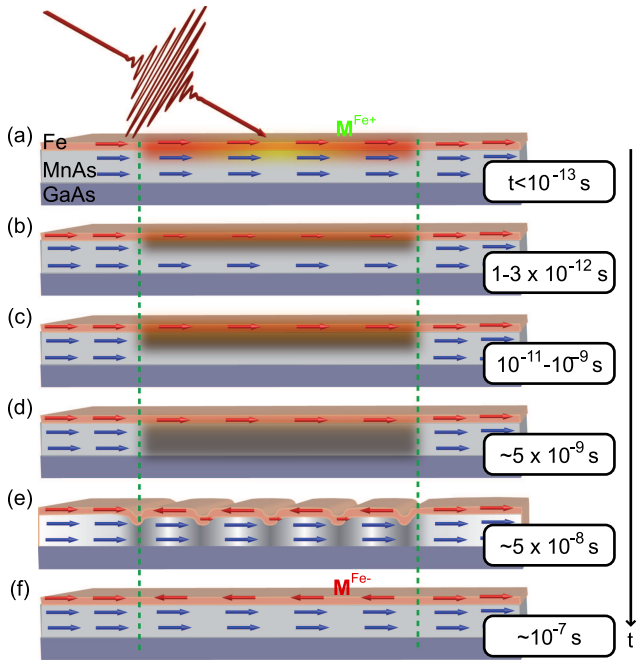

Figure 5 LT14521 03NOV2014